*Acta Cryst.* (1973). A29, 35

# Experimental Methods for the Study of Multiple Borrmann Diffraction*

BY T. C. HUANG† AND B. POST

*Physics Department, Polytechnic Institute of Brooklyn, Brooklyn, New York* 11201, *U.S.A.*

(*Received* 22 *August* 1972; *accepted* 25 *September* 1972)

Relatively simple techniques, utilizing divergent unfiltered microbeam X-ray sources and large source-to-detector (film) distances, have been used to obtain detailed high-resolution photographs of regions of interest in reciprocal space. These photographs reveal many previously unreported intensity anomalies. An example is given of a completely indexed photograph of forward direct beams transmitted through a perfect germanium crystal. Points of interest are discussed.

## Introduction

The observation by Borrmann & Hartwig (1965) that 111 reflections anomalously transmitted through perfect germanium crystals undergo additional enhancement when the $11\bar{1}$ reflection is simultaneously in diffracting position, has stimulated a number of theoretical and experimental investigations of simultaneous Borrmann diffraction effects (Ewald & Heno, 1968; Heno & Ewald, 1968; Joko & Fukuhara, 1967; Hildebrandt, 1967). For the most part these have been concerned with dynamical effects which occur in crystals set at the exact angle for *n*-beam diffraction. The incident beam is generally assumed to be perfectly monochromatic and absolutely non-divergent. Results obtained from these studies have been useful, but they yield little or no information regarding regions of reciprocal space immediately adjacent to the *point* investigated. Since real incident beams always possess finite divergence, it is extremely difficult to make meaningful comparisons between experimental observations and theoretical predictions of the type mentioned. Useful comparisons require averaging over significantly large regions of reciprocal space, within which absorption coefficients, polarizations, and excitations of specific modes of propagation may vary rapidly.

We have for several years utilized relatively simple techniques for investigations of these types. In many instances these reveal effects of considerable interest whose existence had not previously been noted in the literature. A brief description of our experimental methods and some results may be of interest.

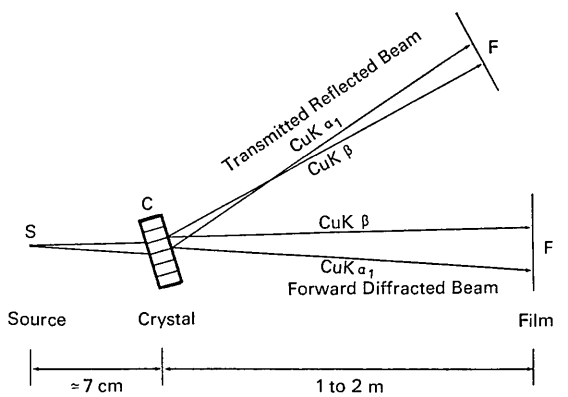


Fig. 1. Schematic diagram of experimental arrangement.

## Experimental

Since our experimental objectives involve the study of regions of reciprocal space near *n*-beam points, good angular resolution has been a primary goal. We achieve this by utilizing microbeam X-ray sources in conjunction with large specimen-to-film distances. Photographic film is used as the detector of diffracted beams to minimize time needed to investigate large areas of reciprocal space and to enable us to record forward diffracted (FD) and transmitted reflected (TR) data simultaneously. The crystal is usually placed as close as possible to the incident divergent unfiltered beam (usually *ca.* 7 cm). The use of a divergent incident beam enormously facilitates the alignment of the crystal. It is only necessary to adjust the crystal to within 2 or 3° of the optimum setting; the divergent beams (*ca.* 8°) will then seek out the effects sought.

While many factors affect angular resolution of recorded data, the major one is the angle subtended by the source at the film. The use of large source-to-film distances (1 to 2 m) enables us to achieve angular resolution of a few sec of arc. Evacuation of the air path

* Research supported in part by the Office of Naval Research under Contract No. N00014-67-A-0438-005.

† Abstracted in part from a dissertation submitted by T. C. Huang to the Polytechnic Institute of Brooklyn in partial fulfillment of the requirements for the degree of Doctor of Philosophy in Physics. Present address: I.B.M. System Products Division, Essex Function, Vermont 05452, U.S.A.

from crystal to film reduces air scattering and cuts down exposure times significantly, especially for longer wavelengths (by a factor of about 4 for Cu $K\alpha$ for a 1 m crystal-to-film distance).

A schematic diagram of our experimental setup is shown in Fig. 1. The relatively short source-to-crystal distance makes possible the interception of the entire divergent incident beam by crystal platelets of moderate size. The use of unfiltered radiation leads to some cluttering up of the films, particularly in the FD direction, but it also makes possible the study of dynamical diffraction effects as function of the wavelength on one film. We will illustrate this below.

## Results

Fig. 2 is a photograph of the FD and the three TR beams diffracted in the four beam ($0\bar{2}2$, $02\bar{2}$, $0\bar{4}0$) case. This was obtained by reducing the crystal-to-film distance to only 5 cm to illustrate the entire recording process.

Fig. 3 is a photograph of the forward direct beam showing multiple Borrmann diffraction of a divergent and polychromatic Cu $K$ incident X-ray beam. A perfect (100) cut germanium crystal was used. The crystal was oriented to diffract the Cu $K\alpha$ radiations for the ($0\bar{2}2, 02\bar{2}, 0\bar{4}0$) four-beam case. Due to the divergence of the incident beam, this setting also enabled us to observe many other multiple diffraction effects, including (111, $11\bar{1}$), (111, $0\bar{2}2$, $1\bar{1}3$) and (111, $02\bar{2}$) *etc.*

In general, the intensities of non-characteristic wavelengths are so low that the corresponding two-beam reflections manifest themselves only as a diffuse background. The intense diffraction lines are portions of Kossel cones for the characteristic radiations, namely Cu $K\alpha_1$, Cu $K\alpha_2$, W $L\alpha_1$, Cu $K\beta$ and W $L\beta_1$, *etc.* These appear as straight lines on photographs where they are simply magnifications of small segments of individual conic sections. Multiple Borrmann effects are displayed at some of the intersections of these Kossel cones when they are due to the same wavelength.

The vertical streak near the center of Fig. 3 marks the trace of a mirror plane of symmetry. This streak arises as a result of $n$-beam enhancements of ($111, 11\bar{1}$) and ($0\bar{2}2, 02\bar{2}, 0\bar{4}0$) for a continuous range of wavelengths. Although the corresponding two-beam reflections are not detectable, at the $n$-beam settings enhancement is strong enough to lead to the formation of the visible streak. The overlap of the three- and four-beam streaks causes confusion in some regions but is separable into its components near the strong characteristic $n$-beam points.

Regions which appear light on the photograph are actually regions of high diffracted intensities. The light area in the lower part of the photograph is due to the two-beam 220 diffraction of continuous Cu radiation (characteristic lines due to the 220 reflection do not appear on Fig. 3). The light region ends abruptly, as we move upward, at the wavelength $\lambda = 1{\cdot}116$ Å (germanium $K$ absorption edge). This edge coincides with the transition from light to dark areas which extends horizontally across the photograph. Other two-beam diffraction effects, namely those due to 111 and $11\bar{1}$, at $\lambda = 1{\cdot}116$ Å are just visible in the upper corners of Fig. 3.

'Deficiency lines' which intersect near the lower part of the vertical streak are the loci of 'eclipses' (Balter, Feldman & Post, 1971; Feldman & Post, 1972) of various $n$-beam cases including the combinations of 111, 220 and 113 reflections at $\lambda = 1{\cdot}405$ Å.

The strongest lines are the $0\bar{2}2$ and $02\bar{2}$ Cu $K\alpha$ and $K\beta$ lines. The Cu $K\alpha_1$ lines were not resolved from Cu $K\alpha_2$ mainly because of the broadening of strong lines on the film due to halation effects. We also observe an intense $0\bar{4}0$ set of lines which run horizontally across the film.

Fig. 4 is a schematic representation of significant features of Fig. 3 including *hkl* indices and wavelengths of most lines. Since a mirror plane bisects the film in the vertical direction, only effects on the right hand side will be discussed.

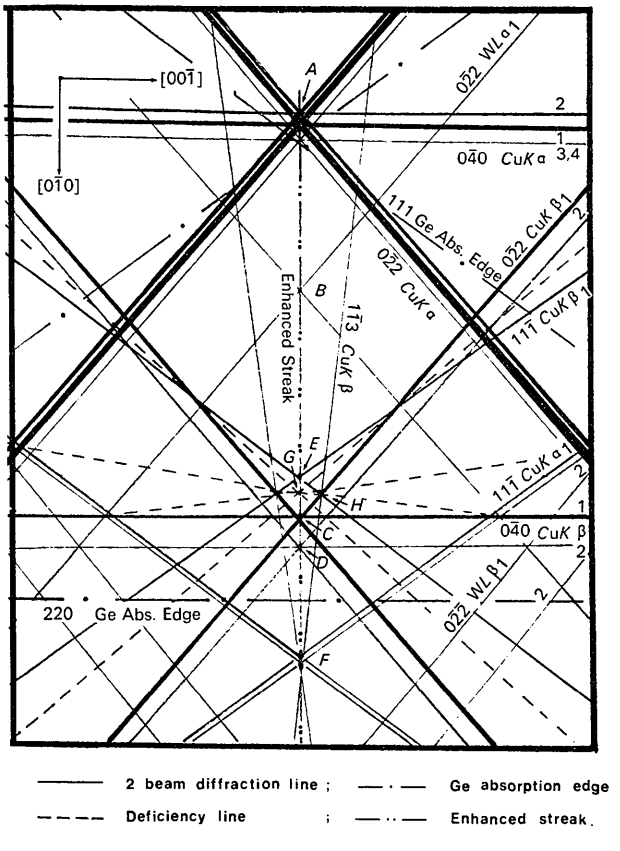


Fig. 4. Schematic indexed representation of Fig. 3.

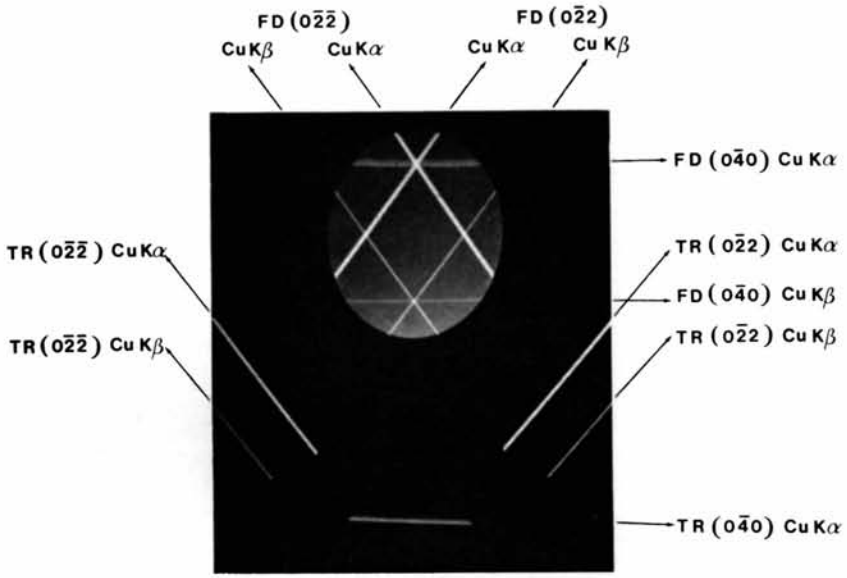


Fig. 2. Divergent-beam transmission photograph. (100) cut germanium ($t=0{\cdot}5$ mm) showing forward diffracted (FD) and transmitted reflected (TR) beams. (25 kV, 2 mA, crystal-to-film distance 5 cm, exposure time 5 min).

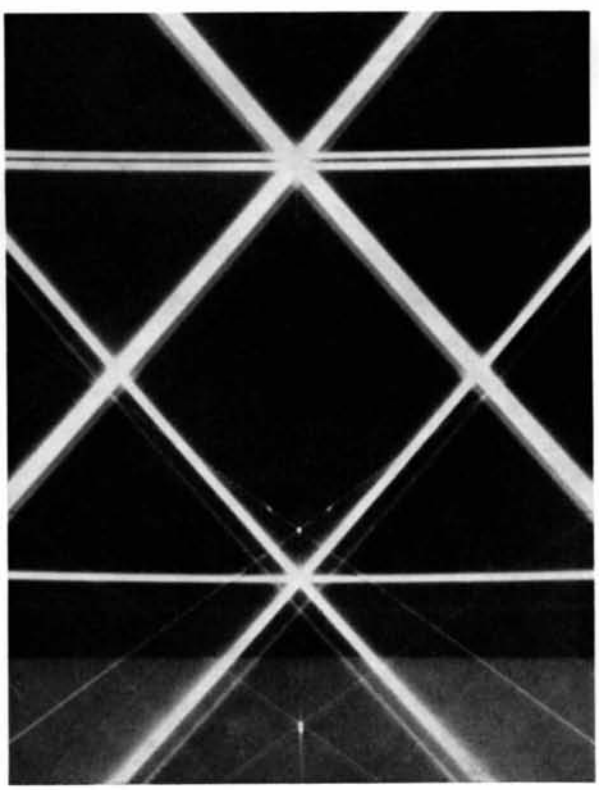

Fig. 3. Forward diffracted divergent-beam photograph. (100) cut germanium crystal ($t=0{\cdot}5$ mm, 25 kV, 2 mA, crystal-to-film distance 100 cm, exposure time 16 hrs).

[*To face p.* 36

Four-beam ($0\bar{2}2$, $02\bar{2}$, $0\bar{4}0$) points due to characteristic wavelengths appear along the vertical symmetry line. The point due to Cu $K\alpha$ appears at $A$; that due to W $L\alpha$ appears at $B$. Diffraction by W $L\alpha$ occurs because of tungsten contamination of the surface of the copper target. The $0\bar{4}0$ W $L\alpha$ two-beam line is too weak to be observed on this photograph, but $0\bar{2}2$ and $02\bar{2}$ are clearly visible. Additional four-beam points, due to Cu $K\beta_1$ and Cu $K\beta_2$, appear at $C$ and $D$. The Cu $K\beta$ lines appear more intense than the corresponding Cu $K\alpha$ lines because for both two- and three-beam reflections in germanium, Cu $K\beta$ is absorbed significantly less than Cu $K\alpha$ (Balter, 1971).

The satellite Cu $K\alpha_3$ and Cu $K\alpha_4$ lines of $0\bar{2}2$ show up clearly and the corresponding $0\bar{4}0$ lines can also be detected on the short wavelength side of the corresponding Cu $K\alpha_1$ line [$\lambda$(Cu $K\alpha_{3,4}$) = 1·534 Å].

Enhanced three-beam (111, $11\bar{1}$) points also appear along the vertical symmetry line at $E$ (Cu $K\beta$) and $F$ (Cu $K\alpha_1$ and $\alpha_2$).

Several additional enhanced three-beam points appear on the photograph. These will be omitted from the discussion in favor of two particularly interesting cases.

The (111, $11\bar{1}$, $0\bar{2}2$, $02\bar{2}$, $0\bar{4}0$, $1\bar{1}3$, $1\bar{1}\bar{3}$) eight-beam point at 1·405 Å shows moderate enhancement at the exact $n$-beam point at $G$. Balter (1971) has shown that this eight-beam point can occur only at this wavelength. Just beneath the enhanced point (a few mm below the three-beam Cu $K\beta_1$ at $E$) is an interesting 'eclipse' point. This involves the intersection of six 'deficiency lines': those due to ($0\bar{2}\bar{2}$, $11\bar{1}$), ($0\bar{2}\bar{2}$, $11\bar{1}$, $1\bar{1}\bar{3}$), ($0\bar{2}2$, 111, $1\bar{1}\bar{3}$), (111, $0\bar{4}0$), ($0\bar{2}\bar{2}$, 111) and ($11\bar{1}$, $0\bar{4}0$). Finally, at $H$ we observe the four-beam (022, 111, $1\bar{1}3$) point due to Cu $K\beta_1$, mistakenly labeled a three-beam point by Katsnel'son, Kisin & Polyakova (1969). On less highly over-exposed photographs an 'eclipse' can be seen to pass through the intersection of the strong $0\bar{2}2$ and 111 lines due to Cu $K\beta_1$. The continuation of this 'eclipse' as a function of wavelength, manifests itself on the photograph as a 'deficiency line' to the right of $H$. Also, close examination reveals the relatively faint, but still detectable, $1\bar{1}3$ line which Iveronova, Katsnel'son, Borodina & Sapkova (1972) had stated could not be detected on $n$-beam Borrmann photographs.

Although we shall present quantitative discussions of these $n$-beam effects elsewhere, it should be noted here that we have been able to account for all the effects listed above on the basis of the plane-wave dynamical diffraction theory of Ewald (1917) as modified by Laue (1931) and as extended for $n$-beam cases by Kato (1958).

## References


BALTER, S. (1971). Doctoral Dissertation, P.I.B., Brooklyn, N.Y.

BALTER, S., FELDMAN, R. & POST, B. (1971). *Phys. Rev. Letters*, **27**, 307–310.

BORRMANN, G. & HARTWIG, W. (1965). *Z. Kristallogr.* **121**, 401–409.

EWALD, P. P. (1917). *Ann. Phys.* **54**, 519–597.

EWALD, P. P. & HENO, Y. (1968). *Acta Cryst.* A**24**, 5–15.

FELDMAN, R. & POST, B. (1972). *Phys. Stat. Sol.* (*a*)**12**, 273–276.

HENO, Y. & EWALD, P. P. (1968). *Acta Cryst.* A**24**, 16–42.

HILDEBRANDT, G. (1967). *Phys. Stat. Sol.* **24**, 245–261.

IVERONOVA, V. I., KATSNEL'SON, A. A., BORODINA, T. I. & SAPKOVA, I. G. (1972). *Phys. Stat. Sol.* (*a*)**11**, 39–44.

JOKO, T. & FUKUHARA, A. (1967). *J. Phys. Soc. Japan*, **22**, 597–604.

KATO, N. (1958). *Acta Cryst.* **11**, 885–887.

KATSNEL'SON, A. A., KISIN, V. I. & POLYAKOVA, N. A. (1969). *Sov. Phys. Crystallogr.* **6**, 965–968.

LAUE, M. VON (1931). *Ergeb. Exakt. Naturwiss.* **10**, 133–158